A mechanism for ATP-sensitive potassium channel diversity: Functional coassembly of two pore-forming subunits

Yi Cui*, Jonathan P. Giblin*, Lucie H. Clapp, and Andrew Tinker[†]

Centre for Clinical Pharmacology, Department of Medicine, University College London, The Rayne Institute, 5 University Street, London WC1E 6JJ, United Kingdom

ATP-sensitive potassium channels are an octomeric complex of four pore-forming subunits of the Kir 6.0 family and four sulfonylurea receptors. The Kir 6.0 family consists of two known members, Kir 6.1 and Kir 6.2, with distinct functional properties. The tetrameric structure of the pore-forming domain leads to the possibility that mixed heteromultimers may form. In this study, we examine this by using biochemical and electrophysiological techniques after heterologous expression of these subunits in HEK293 cells. After the coexpression of Kir 6.1 and Kir 6.2, Kir 6.1 can be coimmunoprecipitated with isoform-specific Kir 6.2 antisera and vice versa. Coexpression of SUR2B and Kir 6.2 with Kir 6.1 dominant negatives at a 1:1 expression ratio and vice versa led to a potent suppression of current. Kir 6.1, and Kir 6.2 dominant negative mutants were without effect on an inwardly rectifying potassium channel from a different family, Kir 2.1. Single-channel analysis, after coexpression of SUR2B, Kir 6.1, and Kir 6.2, revealed the existence of five distinct populations with differing single-channel current amplitudes. All channel populations were inhibited by glibenclamide. A dimeric Kir 6.1–Kir 6.2 construct expressed with SUR2B had a single-channel conductance intermediate between that of either Kir 6.2 or Kir 6.1 expressed with SUR2B. In conclusion, Kir 6.1 and Kir 6.2 readily coassemble to produce functional channels, and such phenomena may contribute to the diversity of nucleotide-regulated potassium currents seen in native tissues.

Both the voltage-gated (K_v) and inwardly rectifying family (K_{ir}) of potassium channel are tetrameric proteins with a large number of family members (1). The cloned members of the inwardly rectifying family of potassium channels form a number of currents that have key physiological functions (2). The tetrameric structure of K^+ channels leads to the possibility of coassembly to form unique heteromultimeric channels. Indeed, with the voltage-gated family, there is good evidence that coassembly can largely occur only between the subfamily members but not between different subfamilies and is determined by an N-terminal compatibility domain (3). In addition, such coassembly occurs in heterologous and native systems and contributes to the diversity of functional properties of voltage-gated potassium channels (4–7). In contrast, the picture with inwardly rectifying potassium channels is more complex. Channels can exist largely as homomultimers in heterologous expression systems and native tissue despite the expression of other subfamily members in the same cell (8, 9) and as heteromultimers, in which the major functional component is a mixture (10).

ATP-sensitive potassium channels have a key role in linking metabolism to electrical excitability and control processes such as insulin release from the pancreatic β cell (11). The ATP-sensitive potassium channel is an octomeric protein complex composed of two subunit types, namely a pore forming subunit (Kir 6.1, Kir 6.2) and the sulfonylurea receptor subunit (SUR1, SUR2A, SUR2B), a member of the ATP-binding cassette transporter family of proteins. The assembly of a particular pore-forming subunit with a particular SUR generates currents with a characteristic single-channel conductance, nucleotide regulation, and pharmacology (12–15). It is clear that, in some settings, the cloned currents are essentially equivalent to the native current; for example, the combination of Kir 6.2 and SUR1 is very like the channel native to the pancreatic β cell. However, in others tissues, most notably smooth muscle, there are discrepancies (16). A key issue is whether mixed heteromultimeric populations can occur with this important channel subfamily. If functional, these might be expected to have hybrid properties. In this study, we show that heteromultimerization occurs readily between Kir 6.1 and Kir 6.2 and results in functional channel populations with differing single-channel conductances.

Methods

Molecular Biology. Standard subcloning techniques were used throughout. SUR1, SUR2A and SUR2B, Kir 6.1 were expressed in pcDNA3 (Invitrogen) and Kir 6.1, Kir 6.2 and Kir 2.1-His6 in pcDNA3.1/Zeo (Invitrogen). Mutations were introduced into Kir 6.1 and Kir 6.2 by using the QuickChange kit (Stratagene) according to manufacturer's instructions. A Kir 6.1–Kir 6.2 dimer was constructed based on a Kir 6.1-green fluorescent protein (GFP) construct. The latter was generated by subcloning a BamHI/EcoRI fragment of Kir 6.1 into the BglII/EcoRI site of pEGFP-N1 (CLONTECH). A PCR fragment was generated by using a high fidelity polymerase (Vent DNA polymerase; New England Biolabs) corresponding to the remaining coding sequence of Kir 6.1 without the stop codon and in-frame with GFP. This fragment was then subcloned into the above with an EcoRI/ApaI digest to give Kir 6.1-GFP in pEGFP-N1. Kir 6.2 was amplified as above by using PCR to include a BamHI and NotI site. The latter digest was then used to fuse Kir 6.2 in-frame with Kir 6.1 by replacing enhanced GFP (EGFP) in the vector. The final product and Kir 6.1-GFP were sequenced to confirm their identity.

Cell Culture and Transfection. HEK293 cells were cultured and transfected, and stable cell lines expressing SUR2B + Kir 6.1, SUR2A + Kir 6.2, SUR2B + Kir 6.2, or Kir 6.1 + Kir 6.2 were generated as previously described (17). For the dominant negative experiments, HEK293 cells were transfected with wild-type Kir 6.x and mutant cDNA in a 1:1 ratio (0.2 μg wild type and 0.2 μg mutant) together with SUR2B cDNA (0.4 μg). For single-channel recording, the Kir 6.1 + Kir 6.2 stable cell line was transfected with 0.4 μg SUR2B cDNA. For electrophysiological recording, GFP cDNA (50–100 ng, EGFPN1; CLONTECH) was cotransfected to enable transfected cells to be identified by epifluorescence.

Antiserum Production in Rabbits. Peptides corresponding to the C terminus of Kir 6.1 (RRNNSSLMVPKVQFMTPEGNQC) and both the N terminus (EEYVLTRLAEDPAEPRYRC) and the C terminus of Kir 6.2 (DALTLASSGPLRKRSC) were synthesized and linked to keyhole limpet hemocyanin before injection into rabbits by using standard protocols (Regal Group, Surrey, U.K.). Bleeds were assayed for activity by using a standard ELISA assay, and bleeds showing reactivity were affinity purified.

Covalent Coupling of Antibodies to Protein A Sepharose. Approximately 10 μg of affinity-purified antibody in TBS at a concentration of 10 μg/ml was incubated with 10 mg protein A Sepharose CL-4B (Amersham Pharmacia) at room temperature for 1 h with gentle rotation. The Sepharose pellet was collected by centrifugation and washed twice with coupling buffer (200 mM sodium borate, pH 9.0). After washing, the pellet was resuspended in coupling buffer containing 20 mM dimethylpimelimidate and incubated for 30 min with gentle rotation. The reaction was stopped by collecting the Sepharose pellet by centrifugation and washing with stop buffer (200 mM ethanolamine, pH 8.0). The Sepharose pellet was then incubated for a further 2 h in stop buffer at room temperature with gentle rotation. The pellet was harvested by centrifugation and washed with 100 mM glycine (pH 3.0) to remove any antibody molecules noncovalently bound. The washed pellet was then resuspended in TBS to produce a 1:1 suspension.

Gel Electrophoresis and Immunoprecipitation. SDS/PAGE Western blotting and immunoprecipitation were carried out as previously described (17).

Immunofluorescence. Cells were plated onto multispot glass microscope slides (pretreated with a 0.01% solution of Poly(L)-Lysine). All subsequent steps were done at 4°C unless otherwise stated. Cell-coated slides were washed in PBS before incubation with 4% (vol/vol) formaldehyde solution. Slides were then given two washes (10 min/wash) with large volumes of PBS before a 20-min permeabilization step with PBS + 0.2% Triton X-100. Slides were washed twice with PBS and then incubated with blocking solution (2% BSA, 5% goat serum, 0.1% Triton X-100 in PBS) for 1 h. Primary and secondary antibodies were prepared in blocking solution at the dilutions indicated and centrifuged for 10 min at 20,800 × g to remove any aggregated material. After blocking, 50 μl of affinity-purified primary antibody (1:500 dilution) was layered onto the slide and incubated for 1 h followed by four washes with PBS. A 1:300 dilution of secondary antibody (Rhodamine red conjugated goat anti-rabbit IgG; Molecular Probes) was then applied to the slide in a 50-μl volume and incubated for 1 h at room temperature. After a final set of four washes with PBS, the slides were air dried and mounted with Vectashield (Vector Laboratories). Slides were viewed and analyzed by using a computer-based image analysis system (OPENLAB 3.1; Improvision, Cambridge, U.K.) coupled to a Zeiss Axiovert 100 M microscope equipped with epifluorescence illumination and appropriate filter sets (Omega Optical, Brattleboro, VT).

Electrophysiology. Whole-cell and cell-attached patch–clamp recordings were performed by using an Axopatch 200B amplifier (Axon Instruments, Foster City, CA). Current signals were filtered at 1–2 kHz and digitized at 5 kHz by using Digidata 1200 interface and analyzed by using PCLAMP software (Axon Instruments) and SATORI V3.2 (Intracel, Coventry, U.K.). Patch pipettes were pulled and fire polished by using a DMZ-universal puller (Zietz Instruments, Germany). Pipettes had resistances of 1.5–3 MΩ for whole-cell recordings and 6–9 MΩ for cell-attached recordings. The capacitance of pipettes was reduced by coating pipettes with a parafilm/mineral oil suspension and compensated for electronically. Series resistance during whole-cell recording was compen-
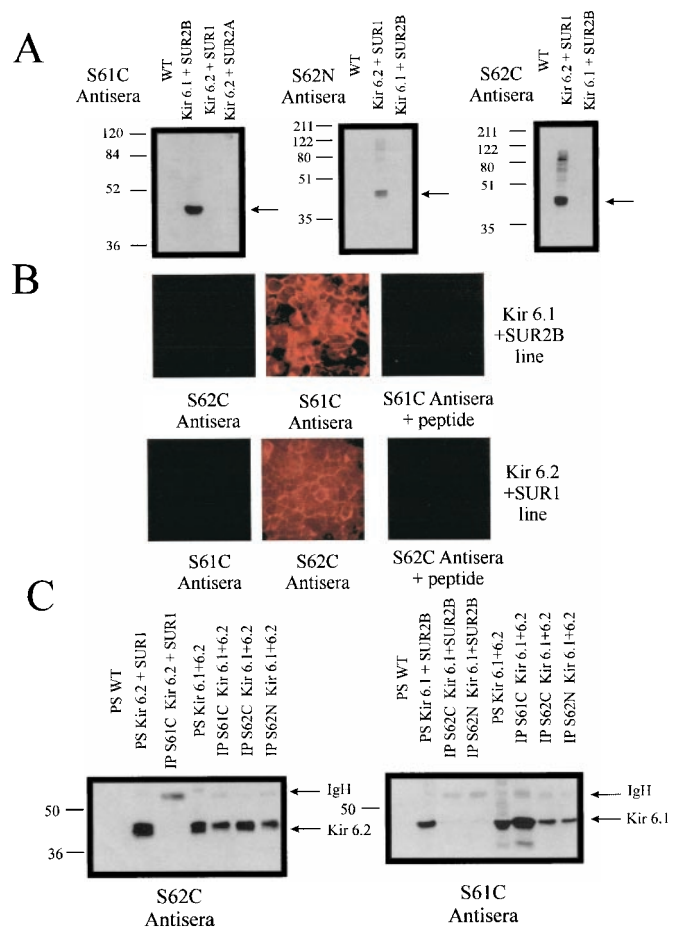

Fig. 1. Characterization of antisera by Western blotting and immunofluorescence and coimmunoprecipitation of Kir 6.1 and Kir 6.2. (*A*) Western blots characterizing Kir 6.0 subtype antisera. Samples were run on a 10% (S61C probed blot) or a 12% (S62C/N probed blot) denaturing polyacrylamide gel. The amount of each sample loaded was 3.5 μg, and all blots were exposed to film for 30 s. The position of the Kir 6.0 subtype is indicated by the arrows, and the molecular weight markers are shown alongside the blots. Kir 6.1 migrates as an approximately 48-kDa protein and Kir 6.2 migrates as an approximately 44-kDa protein. The lanes labeled WT denote untransfected HEK293 cells. (*B*) Characterization of immunofluorescence against the Kir 6.1 + SUR2B and the Kir 6.2 + SUR1 lines. Immunofluorescent staining and analysis was as described in *Methods*. The subtype specificity of immunostaining and competition with the immunogenic peptide (1 mg/ml) can be observed. (*C*) On the *Left*, a Western blot (from a 12% denaturing polyacrylamide gel) probed with the S62C antisera. From *Left* to *Right*, the first three lanes show that Kir 6.2 is present in the SUR1 + Kir 6.2 cell line (PS, protein sample) and that the Kir 6.1C antiserum does not immunoprecipitate Kir 6.2. The next four lanes show immunoprecipitation studies done on a stable line coexpressing Kir 6.1 and Kir 6.2. As expected, Kir 6.2 is immunoprecipitated by both S62C and S62N, but Kir 6.2 is also coimmunoprecipitated by the S61C antiserum. On the *Right*, a Western blot (from a 10% denaturing polyacrylamide gel) probed with the S61C antisera. From *Left* to *Right*, the first four lanes show that Kir 6.1 is present in the SUR2B + Kir 6.1 cell line (PS, denatured protein sample homogenate taken before IP) and that the S62N and S62C antiserum do not immunoprecipitate Kir 6.1. The next four lanes show the samples of homogenate and immunoprecipitation reactions from the Kir 6.1 + Kir 6.2 stable line, and they show that Kir 6.1 is immunoprecipitated by the S61C antiserum and also coimmunoprecipitated by the S62C and S62N antisera (same samples as exposed to the S62C antisera on the *Left*). Both Western blots were exposed to film for 30 s. The positions of Kir 6.1, Kir 6.2, and the Ig heavy chain (IgH, only a small amount present because of the covalent linkage to protein A) are indicated by the black arrows. Molecular weight markers are shown alongside the blots.

sated to at least 75% by using the amplifier. The pipette solution contained (in mM): 107 KCl, 1.2 MgCl$_2$, 1 CaCl$_2$, 10 EGTA, 5 Hepes (with 33 mM KOH to pH 7.2) and the bath solution; 140 KCl, 2.6 CaCl$_2$, 1.2 MgCl$_2$, 5 Hepes (pH 7.4) For data shown in Figs. 4 and 5, single-channel current amplitudes were measured by constructing amplitude histograms. The data were fitted with a twin peak Gaussian function, and the two peaks were subtracted to obtain the current amplitude. On a few occasions, the Gaussian function did not converge well, and, in this case, the two main peaks were subtracted. For the data shown in Fig. 4D, a mean current amplitude was measured over a 20-s recording period. Statistical analysis was carried out by using one-way ANOVA or Student's t test as appropriate (ORIGIN V6.0). Statistical significance is as indicated in the legend and text. Data are presented as mean ± SEM.

Results

We first set out to investigate the ability of Kir 6.1 and Kir 6.2 to interact by using biochemical assays. A number of rabbit antisera were generated to peptides corresponding to regions in the N and C terminus of Kir 6.2 (S62N and S62C) and the C terminus of Kir 6.1 (S61C). We first tested the ability of these antisera to specifically recognize Kir 6.1 and Kir 6.2 in control HEK293 cells and in stable lines expressing Kir 6.2 and SUR1, Kir 6.2 and SUR2A, and Kir 6.1 and SUR2B. Fig. 1A shows that the antisera recognize proteins of the predicted molecular weight by immunoblotting. Dot blots to the relevant peptide show equivalent sensitivity of the two antisera used in Fig. 1A, S62C and S61C (not shown). The comparable intensity of the signal from the lysate indicates that Kir 6.1 and Kir 6.2 are expressed at approximately the same level in the Kir 6.1/6.2 stable line. Fig. 1B shows that two of the antisera (S61C and S62C) lead to specific immunofluorescence. The antiserum raised to the N terminus of Kir 6.2 (S62N) was also selective when tested in an analogous fashion (not shown). The antisera were next used to test the potential for Kir 6.1 and Kir 6.2 to interact biochemically by using a coimmunoprecipitation strategy. Covalent coupling of the antisera to protein A avoids problems of recognition of the heavy chain by the secondary antibody. Fig. 1C shows that, in a monoclonal stable line expressing both Kir 6.1 and Kir 6.2, immunoprecipitation of Kir 6.1 by S61C resulted in copurification in immune complexes of Kir 6.2. In a reciprocal fashion, immunoprecipitation of Kir 6.2 by both S62N and S62C resulted in the copurification of Kir 6.1. In each case, the coimmunoprecipitation was judged to be meaningful, as Kir 6.1 was not immunoprecipitated from the SUR2B + Kir 6.1 stable line by S62N or S62C (Fig. 1C) but S61C could (not shown), and Kir 6.2 was not immunoprecipitated from the SUR2A + Kir 6.2 stable line by S61C (Fig. 1C) but S62N and S62C could (not shown). The experiment shown in Fig. 1C was repeated on at least two other occasions with similar results. On two of the four occasions during immunoprecipitation with S62N and S62C from the Kir 6.1 + SUR2B line, prolonged exposure of the blot (>5 min) revealed a band of similar but slightly higher mobility than Kir 6.1. However, with shorter exposures, the data in Fig. 1C clearly show specific and robust coimmunoprecipitation of the heterologously expressed components.

The tetrameric nature of potassium channels gives the potential to explore interactions between subunits by using a functional dominant negative assay (18). The dominant negative effect arises because a mutant nonfunctional subunit can inactivate the function of wild-type subunits in a tetramer. Thus, mutations were introduced into the conserved GFG sequence in the pore of Kir 6.1 (GFG to AFA; 61GA and GFG to SFG; 61GS) and Kir 6.2 (GFG to AFA; 62GA) (19, 20). To ensure potentially equal expression of wild-type and mutant subunits, these constructs were transfected transiently at equal concentration together with SUR2B, and whole-cell membrane currents were recorded by using the patch–clamp technique. SUR2B is the putative smooth muscle sulfonyl-urea receptor (21). Fig. 2 shows the effect of coexpression of 61GA,
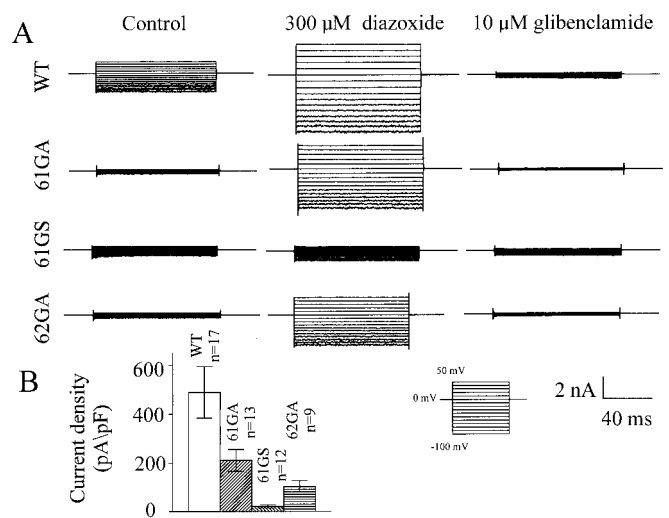

Fig. 2. Dominant negative effects of 61GA, 61GS, and 62GA on SUR2B + Kir 6.1 current expression. (A) Whole-cell current traces recorded from cells transiently transfected with SUR2B + Kir 6.1 (WT), SUR2B + Kir 6.1 + 61GA (61GA), SUR2B + Kir 6.1 + 61GS (61GS), or SUR2B + Kir 6.1 + 62GA (62GA) under the control conditions (5 min after breakin), in the presence of diazoxide (300 μM) and glibenclamide (10 μM), respectively. The pipette solution (see *Methods*) was supplemented with 0.5 mM GDP. (B) Summarized data for the currents measured at −100 mV. $P < 0.01$ one-way ANOVA.

61GS, and 62GA on Kir 6.1 + SUR2B currents. Potassium-selective currents were recorded in symmetrical potassium solutions (see *Methods*) with 0.5 mM GDP in the pipette, the inclusion of which resulted in current run-up over a 5-min period. Under these conditions, however, Kir 6.1 + SUR2B currents were increased further by the application of the potassium channel opening drug, diazoxide and almost totally blocked by the sulfonylurea,
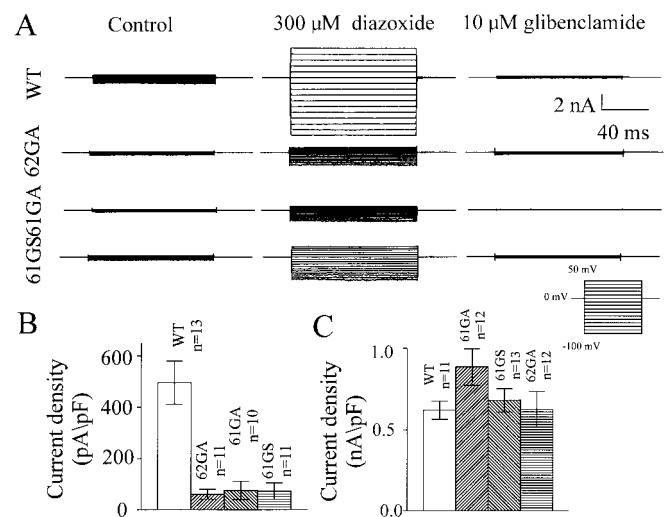

Fig. 3. Dominant negative effects of 62GA, 61GA, and 61GS on SUR2B + Kir 6.2 current. (A) Whole-cell current traces recorded from cells transiently transfected with SUR2B + Kir 6.2 (WT), SUR2B + Kir 6.2 + 62GA (62GA), SUR2B + Kir 6.2 + 61GA (61GA), or SUR2B + Kir 6.2 + 61GS (61GS) under the control conditions (5 min after breakin), in the presence of diazoxide (300 μM) and glibenclamide (10 μM), respectively. The pipette solution (see *Methods*) was supplemented with 3.0 mM ATP. (B) Summarized data for the currents measured at −100 mV. $P < 0.01$, one-way ANOVA. (C) Mean measured currents at −100 mV recorded from cells transiently transfected with Kir 2.1–His6 and cotransfected with Kir 2.1–His6 and the indicated Kir 6.0 constructs (5 min after breakin).
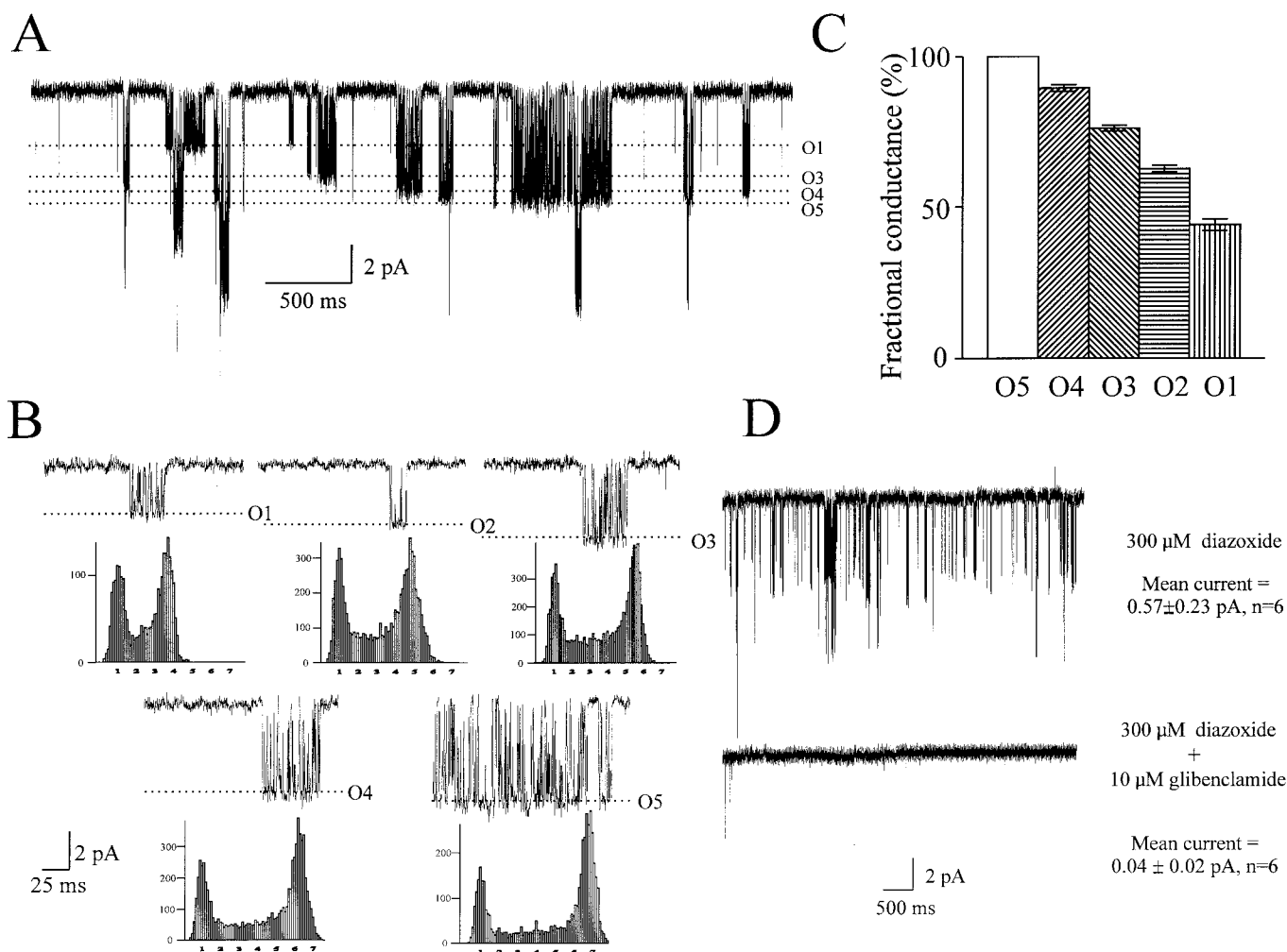
Fig. 4. Five different conductance channels in cells coexpressing SUR2B, Kir 6.1, and Kir 6.2. (*A*) Single-channel current trace (cell-attached configuration) recorded at −100 mV in the presence of 300 μM diazoxide from Kir 6.1 + Kir 6.2 stable cell line transiently transfected with SUR2B. (*B*) Representative recordings of five single channel unitary currents (O1–O5) at −100 mV in the presence of 300 μM diazoxide and their corresponding amplitude histograms. (*C*) Bar chart showing fractional current amplitudes normalized to the O5 channel conductance. (*D*) Pharmacological sensitivity of single-channel currents recorded from Kir 6.1 + Kir 6.2 stable cell line transiently transfected with SUR2B. The current amplitude was measured as a mean current over 20 s recorded at −100 mV and significantly reduced in the presence of 10 μM glibenclamide (*P* < 0.05, paired *t* test).

glibenclamide. The mean data are summarized in Fig. 2*B*. Current densities were calculated at −100 mV as the difference between the diazoxide-stimulated and glibenclamide-inhibited current. 61GA, 61GS, and 62GA all led to a >50% reduction in current compared with control, with 62GA being intermediate in potency (*P* < 0.01, one-way ANOVA). Fig. 3 shows an analogous set of experiments performed after the transient expression of Kir 6.2 + SUR2B alone or together with 61GA, 61GS, and 62GA. Kir 6.2 + SUR2B currents were recorded after dialysis of the cell with a pipette solution containing 3 mM ATP, and current densities were calculated as above. 61GA, 61GS, and 62GA all led to a prominent dominant negative effect when coexpressed at an equivalent concentration (Fig. 3*B*; *P* < 0.01, one-way ANOVA).

Two potential complicating factors influence the interpretation of these experiments. First, these mutants may exert their effects through nonspecific interactions, for example, by saturating the ability of the cell to synthesize protein. Consequently, we tested the ability of these mutants to suppress currents from an inward rectifier from a different subfamily, namely Kir 2.1. A hexahistidine-tagged Kir 2.1 that expresses well in mammalian cells was used. We have previously shown this to have no interaction with Kir 6.1 (8). The mean data shown in Fig. 3*C* indicate that there is no reduction

of current on coexpression with 61GS, 61GA, and 62GA (*P* > 0.05, one-way ANOVA). The coexpression of a sulfonylurea receptor together with a Kir 6.0 is necessary to produce membrane currents. Full-length Kir 6.0 does not traffic to the plasma membrane in the absence of a SUR. Second, it is possible that the mutants may produce the dominant negative effect by interacting with SUR2B and preventing the delivery of wild-type Kir 6.0 subunit to the plasma membrane. To address this, SUR2B was expressed at twice the concentration. If the provision of SUR2B were limiting, it should relieve the dominant negative effect. However, coexpression of 61GS with Kir 6.1 and SUR2B still led to a pronounced reduction in current (SUR2B + Kir 6.1 = 721 ± 197 pA/pF; SUR2B + Kir 6.1 + 61GS = 70 ± 33 pA/pF; *n* = 6, *P* < 0.01, unpaired *t* test).

The information presented so far suggests that Kir 6.1 and Kir 6.2 are able to interact, but it does not address the issue of whether this assembly produces current. In other words, do Kir 6.1/Kir 6.2 heteromultimers result in functional channels? It has been established that Kir 6.2 has a single-channel conductance of ≈70 pS and Kir 6.1 of 35 pS in high (≈150 mM) symmetrical K$^+$ (22, 23). Thus, if coassembly between Kir 6.1 and Kir 6.2 were productive, then conductances intermediate in value between these figures might be expected. To examine this, single-channel recordings were made in
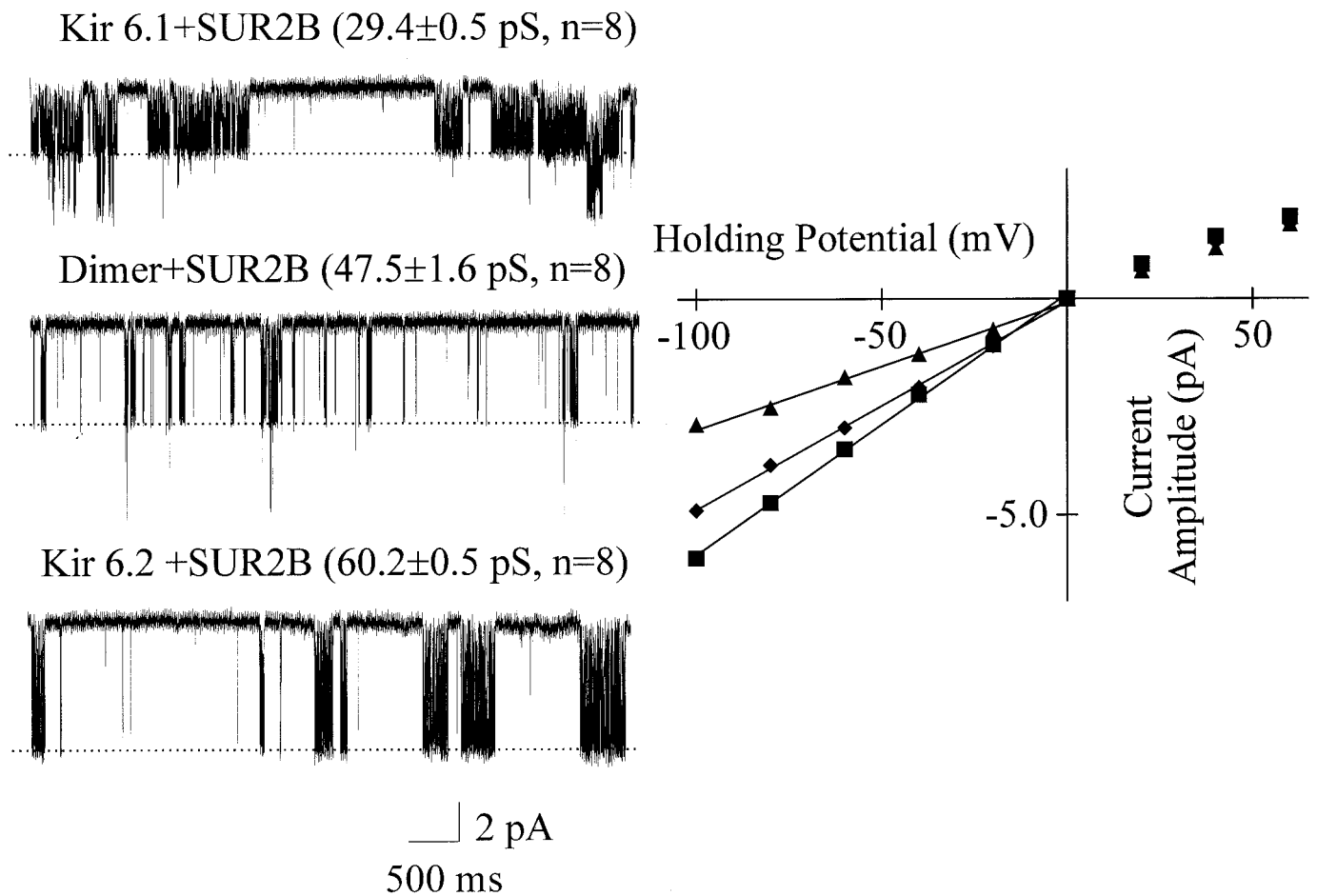
Cui *et al.*

Kir 6.1+SUR2B (29.4±0.5 pS, n=8)

Dimer+SUR2B (47.5±1.6 pS, n=8)

Holding Potential (mV)

Kir 6.2 +SUR2B (60.2±0.5 pS, n=8)

2 pA

500 ms

Fig. 5. Single-channel conductances of SUR2B + Kir 6.1, SUR2B + Kir 6.1–6.2 dimer and SUR2B + Kir 6.2 currents. On the *Left*, single-channel current traces (cell-attached configuration) recorded at −100 mV from SUR2B + Kir 6.1and SUR2B + Kir 6.2 stable cell lines and cells transiently transfected with SUR2B + Kir 6.1—Kir 6.2 dimer in the presence of 300 μM diazoxide. The single-channel conductances shown are significantly different ($P < 0.01$, one-way ANOVA). On the *Right*, the current–voltage relationships of SUR2B + Kir 6.1 (▲), SUR2B + Kir 6.1–Kir 6.2 dimer (♦), and SUR2B + Kir6.2 (■) currents.

the cell-attached configuration in the presence of 300 μM diazoxide in the Kir 6.1 + Kir 6.2 stable line transiently transfected with SUR2B. Recordings were made at a holding potential of −100 mV with 140 mM K$^+$ in the bath, and pipette and revealed the existence of five separate species of current amplitudes (Fig. 4). Fig. 4A shows a trace in which four of these are identifiable and shows the tendency of these to occur in bursts of openings. Fig. 4B shows single-channel recordings with a shorter time base together with examples of the relevant amplitude histogram for each conductance species compiled from a single experiment. Fig. 4C shows the fractional amplitudes normalized to the largest conductance from a number of experiments ($P < 0.01$, one-way ANOVA). The mean currents are O1 = −2.58 ± 0.10 pA, O2 = −3.67 ± 0.05 pA, O3 = −4.46 ± 0.05 pA, O4 = −5.25 ± 0.08 pA, and O5 = −5.87 ± 0.11 pA ($n = 6$, $P < 0.01$, one-way ANOVA). Next, we examined the response of this population of conductances to 300 μM diazoxide in the presence and absence of 10 μM glibenclamide. Currents under the latter condition were essentially abolished with no species of amplitude appearing resistant (Fig. 4D).

It is an appealing possibility that the five current amplitudes observed corresponded, from largest to smallest conductance, to: four Kir 6.2, three Kir 6.2/one Kir 6.1, two Kir 6.2/two Kir 6.1, one Kir 6.2/three Kir 6.1, and four Kir 6.1. One strategy to test this would be to physically constrain the stoichiometry by constructing a dimer linking Kir 6.1 to Kir 6.2. The lone expression of such a construct would largely be expected to constrain the stoichiometry

to two Kir 6.2/two Kir 6.1. Such a construct was made and expression of the cDNA together with that of SUR2B in HEK293 cells resulted in functional channels. A comparison was made between the single-channel conductance of lines stably expressing Kir 6.1 + SUR2B and Kir 6.2 + SUR2B and transient transfection of the dimer together with SUR2B. Single-channel current amplitudes were measured at a series of holding potentials in the cell-attached mode in the presence of 300 μM diazoxide (Fig. 5). The data show that the dimer has a conductance ≈79% that of the Kir 6.2 homotetramer. This figure agrees closely with the O3 fractional conductance values shown in Fig. 4C (76%). Our single-channel conductances are a little lower than the 35 and 70 pS quoted for Kir 6.1 and Kir 6.2 channel forming complexes (22, 23). This may reflect our use of SUR2B and our measurements being performed in the cell-attached configuration combined with a slightly lower potassium concentration.

Discussion

The biochemical and functional data presented here show that it is indeed possible for different pore-forming subunits of the ATP-sensitive potassium channel to coassemble. The interaction of the subunits Kir 6.1 and Kir 6.2 is productive and results in functional channel populations with intermediate single-channel conductance. Is it possible to say how readily this interaction occurs? The electrophysiological studies can give some insight into this. The dominant negative data show that Kir 6.1 dominant negative

constructs (61GS, 61GA) are able to profoundly inhibit both SUR2B + Kir 6.1 and SUR2B + Kir 6.2 currents. In addition, the converse also applies: a Kir 6.2 dominant negative construct (6.2GA) is able to inhibit both SUR2B + Kir 6.1 and SUR2B + Kir 6.2 currents. It is worth stressing that all of the pore-forming cDNAs and mutants are transfected at equal concentration and thus are in a 1:1 ratio. Moreover, by calculating the number of events in the peaks on the amplitude histograms of the various conducting species, one can get some measure of the relative proportion of each species. It is apparent that Kir 6.1 and Kir 6.2 are expressed to a similar level (see *Results*). Performing such analysis, we find that O5:O4:O3:O2:O1 occur in the ratio 1:0.79:0.93:0.64:0.39, and thus we estimate that 63% of the channels are heteromultimers. Therefore, in HEK293 cells, this interaction occurs readily and results in a significant population of heteromultimers.

Does the process of heteromultimerization result in currents with hybrid properties? The major issue addressed in this study is the single-channel conductance. The single channel data with a spectrum of five single-channel conductances in cells coexpressing SUR2B, Kir 6.1, and Kir 6.2 imply that potentially all possible combinations of Kir 6.1 and Kir 6.2 in the homo- and heterotetramer are functional. The response of these heteromultimeric currents to the pharmacological agents glibenclamide and diazoxide argue that regulation mediated through the sulfonylurea receptor is not disrupted. In addition, the dimer of Kir 6.1 and Kir 6.2 has a single-channel conductance intermediate between that of SUR2B + Kir 6.1 and SUR2B + Kir 6.2.

Using a dominant negative assay, Marban and colleagues (20) could find no evidence to support coassembly in a different heterologous expression system (A549 cells) or in cardiac myocytes. However, in their earlier studies, it was noted that a Kir 6.2 dominant negative was able to inhibit K_{ATP} currents in a smooth muscle A10 cell line (24). Furthermore, evidence has been presented for the presence of a small conductance channel in these cells much more in keeping with the potential expression of Kir 6.1 (25). Our conclusions are supported by the work of Zerangue *et al.* (26), who noted using a trafficking assay in *Xenopus laevis* oocytes that Kir 6.1 was able to influence the transport of a Kir 6.2 mutant to the plasma membrane. These observations may not be inconsistent as trafficking of these subunits may differ according to the cellular context. For example, it is possible that Kir 6.1 may be able to form a component of the mitochondrial ATP-sensitive potassium channel in brain, liver, and skeletal muscle (27, 28).

Are there any indications that such coassembly may form meaningful currents in a physiological setting? Both Kir 6.2 and, in particular, Kir 6.1 are widely expressed in a number of tissues, so the potential certainly exists (28–30). It seems very likely that, in some tissues, I_{KATP} is an assembly between four identical SUR subunits and four identical Kir 6.0 subunits. For example, in skeletal and cardiac muscle, the channel is likely to be made up of SUR2A and Kir 6.2, as indicated by the similarities in the single channel conductance and pharmacology of the native and heterologously expressed channel. In such circumstances, if Kir 6.1 is expressed, for example in skeletal muscle, there must be trafficking and/or assembly mechanisms, such as those indicated above, preventing interaction. However, in brain and, in particular, smooth muscle, there seems to be significant heterogeneity in the measured single-channel conductance for the recorded ATP-sensitive potassium currents (11, 16, 31, 32). For example under identical conditions to those used by ourselves (i.e., cell-attached 140 K^+ in the pipette and bath), a 42-pS channel is found in portal vein (33) and a 43-pS channel in urethra (34) that closely corresponds to our O3 conductance (predicted conductance = 44.6 pS). In addition, mimicking the conditions described by other investigators (not shown), we find that some of the described conductances also correspond to both homo- and heteromultimers (35). It is plausible that differences in the relative levels of expression, activation conditions, or other factors may determine which particular subset of homo- or heteromultimers predominate.

We are currently studying the nucleotide regulation of the dimer and Kir 6.1 and Kir 6.2 homomultimers. Other investigators, using dimeric and tetrameric constructs of Kir 6.1 and Kir 6.2, have observed identical ATP sensitivity with one or more Kir 6.2 subunits included in the complex (36, 37). In conclusion, Kir 6.1 and Kir 6.2 readily coassemble to produce functional channels and may contribute to the diversity of nucleotide-regulated currents seen in native tissues.

1. Jan, L. Y. & Jan, Y. N. (1997) *Annu. Rev. Neurosci.* **20**, 91–123.
2. Nichols, C. G. & Lopatin, A. N. (1997) *Annu. Rev. Physiol.* **59**, 171–191.
3. Li, M., Jan, Y. N. & Jan, L. Y. (1992) *Science* **257**, 1225–1230.
4. Isacoff, E. Y., Jan, Y. N. & Jan, L. Y. (1990) *Nature (London)* **345**, 530–534.
5. Sheng, M., Liao, Y. J., Jan, Y. N. & Jan, L. Y. (1993) *Nature (London)* **365**, 72–75.
6. Ruppersberg, J. P., Schroter, K. H., Sakmann, B., Stocker, M., Sewing, S. & Pongs, O. (1990) *Nature (London)* **345**, 535–537.
7. Wang, H., Kunkel, D. D., Martin, T. M., Schwartzkroin, P. A. & Tempel, B. L. (1993) *Nature (London)* **365**, 75–79.
8. Tinker, A., Jan, Y. N. & Jan, L. Y. (1996) *Cell* **87**, 857–868.
9. Raab-Graham, K. F. & Vandenberg, C. A. (1998) *J. Biol. Chem.* **273**, 19699–19707.
10. Krapivinsky, G., Gordon, E. A., Wickman, K., Velimirovic, B., Krapivinsky, L. & Clapham, D. E. (1995) *Nature (London)* **374**, 135–141.
11. Ashcroft, S. J. & Ashcroft, F. M. (1990) *Cell. Signalling* **2**, 197–214.
12. Tucker, S. J. & Ashcroft, F. M. (1998) *Curr. Opin. Neurobiol.* **8**, 316–320.
13. Aguilar-Bryan, L., Clement, J. P., IV, Gonzalez, G., Kunjilwar, K., Babenko, A. & Bryan, J. (1998) *Physiol. Rev.* **78**, 227–245.
14. Babenko, A. P., Aguilar-Bryan, L. & Bryan, J. (1998) *Annu. Rev. Physiol.* **60**, 667–687.
15. Isomoto, S., Kondo, C. & Kurachi, Y. (1997) *Jpn. J. Physiol.* **47**, 11–39.
16. Clapp, L. H. & Tinker, A. (1998) *Curr. Opin. Nephrol. Hypertens.* **7**, 91–98.
17. Giblin, J. P., Leaney, J. L. & Tinker, A. (1999) *J. Biol. Chem.* **274**, 22652–22659.
18. Herskowitz, I. (1987) *Nature (London)* **329**, 219–222.
19. Miki, T., Tashiro, F., Iwanaga, T., Nagashima, K., Yoshitomi, H., Aihara, H., Nitta, Y., Gonoi, T., Inagaki, N., Miyazaki, J., *et al.* (1997) *Proc. Natl. Acad. Sci. USA* **94**, 11969–11973.
20. Seharaseyon, J., Sasaki, N., Ohler, A., Sato, T., Fraser, H., Johns, D. C., O'Rourke, B. & Marban, E. (2000) *J. Biol. Chem.* **275**, 17561–17565.
21. Isomoto, S., Kondo, C., Yamada, M., Matsumoto, S., Higashiguchi, O., Horio, Y., Matsuzawa, Y. & Kurachi, Y. (1996) *J. Biol. Chem.* **271**, 24321–24324.
22. Kondo, C., Repunte, V. P., Satoh, E., Yamada, M., Horio, Y., Matsuzawa, Y., Pott, L. & Kurachi, Y. (1998) *Recept. Channels* **6**, 129–140.
23. Repunte, V. P., Nakamura, H., Fujita, A., Horio, Y., Findlay, I., Pott, L. & Kurachi, Y. (1999) *EMBO J.* **18**, 3317–3324.
24. Lalli, M. J., Johns, D. C., Janecki, M., Liu, Y., O'Rourke, B. & Marban, E. (1998) *Pflugers Arch.* **436**, 957–961.
25. Russ, U., Metzger, F., Kickenweiz, E., Hambrock, A., Krippeit-Drews, P. & Quast, U. (1997) *Br. J. Pharmacol.* **122**, 1119–1126.
26. Zerangue, N., Schwappach, B., Jan, Y. N. & Jan, L. Y. (1999) *Neuron* **22**, 537–548.
27. Suzuki, M., Kotake, K., Fujikura, K., Inagaki, N., Suzuki, T., Gonoi, T., Seino, S. & Takata, K. (1997) *Biochem. Biophys. Res. Commun.* **241**, 693–697.
28. Zhou, M., Tanaka, O., Sekiguchi, M., Sakabe, K., Anzai, M., Izumida, I., Inoue, T., Kawahara, K. & Abe, H. (1999) *Brain Res. Mol. Brain Res.* **74**, 15–25.
29. Inagaki, N., Tsuura, Y., Namba, N., Masuda, K., Gonoi, T., Horie, M., Seino, Y., Mizuta, M. & Seino, S. (1995) *J. Biol. Chem.* **270**, 5691–5694.
30. Karschin, C., Ecke, C., Ashcroft, F. M. & Karschin, A. (1997) *FEBS Lett.* **401**, 59–64.
31. Quayle, J. M., Nelson, M. T. & Standen, N. B. (1997) *Physiol. Rev.* **77**, 1165–1232.
32. Routh, V. H., McArdle, J. J. & Levin, B. E. (1997) *Brain Res.* **778**, 107–119.
33. Cole, W. C., Malcolm, T., Walsh, M. P. & Light, P. E. (2000) *Circ. Res.* **87**, 112–117.
34. Teramoto, N., McMurray, G. & Brading, A. F. (1997) *Br. J. Pharmacol.* **120**, 1229–1240.
35. Zhang, H. L. & Bolton, T. B. (1996) *Br. J. Pharmacol.* **118**, 105–114.
36. Kono, Y., Horie, M., Takano, M., Otani, H., Xie, L. H., Akao, M., Tsuji, K. & Sasayama, S. (2000) *Pflugers Arch.* **440**, 692–698.
37. Babenko, A. P., Gonzalez, G. C. & Bryan, J. (2000) *J. Biol. Chem.* **275**, 31563–31566.